Enhanced Backward-Directed Multiphoton-Excited Fluorescence from Dielectric Microcavities

Steven C. Hill
Army Research Laboratory, 2800 Powder Mill Road, Adelphi, Maryland 20783-1197

Veronique Boutou, Jin Yu, Stephane Ramstein, and Jean-Pierre Wolf
LASIM (UMR5579), Universite Claude Bernard Lyon 1, 43 bd du 11 Novembre, 69622 Villeurbanne Cedex, France

Yong-le Pan
Physical Science Laboratory, New Mexico State University, Las Cruces, New Mexico 88003-8002

Stephen Holler and Richard K. Chang
Department of Applied Physics and Center for Laser Diagnostics, Yale University, New Haven, Connecticut 06520-8284
(Received 28 January 2000)

We demonstrate theoretically and experimentally that one-, two-, and three-photon excited fluorescence from dye molecules in spherical microcavities has an asymmetrical angular distribution and is enhanced in the backward direction. The enhancement ratios (of intensities at 180° and 90°) are 9, 5, and 1.8 for three-, two-, and one-photon excitation, respectively. Even larger ratios are expected for microspheres with an index of refraction larger than that used in the experiments. Because of the reciprocity principle and concentration of the incident wave inside particles, the backward enhancement is expected to occur even with nonspherical particles.

PACS numbers: 33.80.Wz, 33.50.–j, 42.25.Fx, 87.64.Vv

Fluorescence of an ensemble of freely rotating molecules is isotropic. However, when these molecules are homogeneously imbedded in a dielectric microcavity (such as a sphere, spheroid, or cylinder), the emission can become anisotropic. The microcavity can concentrate the internal field intensity $I(\mathbf{r})$ of the incident radiation [1–3], and can introduce an angular-dependent reemission efficiency [4]. Because of the reciprocity principle [5,6], fluorescence from regions of high $I(\mathbf{r})$ tends to return toward the illuminating source. This backward enhancement is expected not only for one-photon [7] but even more so for multiphoton-excited fluorescence (MPEF) that is proportional to $I^n(\mathbf{r})$. The concentration and redirection effect for a spherical particle are analogous to epi-illumination microscopy, where the lens focuses the incident light and directs a large fraction of the fluorescence back toward the source (here the microcavity itself, which is the sample, acts as the lens to focus the incident wave and redirect the fluorescence emission). Microscopy using MPEF has demonstrated improved contrast and resolution [8]. Backward enhancement may be useful for the detection of ultraweak one-photon and especially MPEF from microparticles. The concept should also help in detecting nanocrystals, quantum well structures [9], and possibly even single molecules [10], placed inside or on the surface of a dielectric microcavity, e.g., a glass sphere [11,12]. The effect may call to mind coherent backscattering or weak localization in random media [13]. However, MPEF is not a coherent process (it is emitted spontaneously), and it occurs over a range of wavelengths different from the incident wave.

In this Letter, we demonstrate theoretically and experimentally, for the first time, the existence of backward enhancement of multiphoton-excited fluorescence in microcavities. We show that the enhancement increases with the order n of the multiphoton-excitation process. Specifically, we investigate the angular dependence (from 0° to 180°) of the fluorescence from microdroplets with the same dye, excited by one, two, and three photons. Remarkable enhancement in the backward direction (as much as a factor of 9 relative to the 90° emission for the three-photon excitation process) is both predicted and observed using 100 femtosecond laser pulses. We have calculated that for microspheres, the backward enhancement increases with the refractive index.

The principle of reciprocity [5,6] as applied to this problem implies the following: If a source at $\mathbf{r_a}$ far from the particle generates at $\mathbf{r_b}$ (inside the particle) an intensity that is large relative to intensities at other internal points, then a source at $\mathbf{r_b}$ radiates preferentially toward $\mathbf{r_a}$ (i.e., in the backscattering direction). If the input intensity at $\mathbf{r_b}$ is relatively weak, then a source at $\mathbf{r_b}$ tends to radiate in directions other than $\mathbf{r_a}$. Reciprocity relations are exact only when the excitation and emission wavelengths are identical. When the wavelengths are different [as when the source at $\mathbf{r_b}$ is a fluorescent molecule that reemits longer-wavelength radiation in proportion to $I^n(\mathbf{r})$], the reciprocity principle still tends to imply the angular preferences stated above so long as the refractive index dispersion between the two wavelengths is small.

The total fluorescence power $U_n(\theta_d)$ collected by a detector at angle θ_d (with respect to the incident beam)

 0031-9007/00/85(1)/54(4)$15.00

subtending a differential element of solid angle $d\Omega$ is the sum of the contributions from all molecules in the cavity of volume V,

$$U_n(\theta_d) = \int_V \sigma_n I^n(\mathbf{r})\rho(\mathbf{r}) \times \{F[\mathbf{r}, \theta_d, \mathbf{p}(\mathbf{E}^{\text{int}}(\mathbf{r}))]d\Omega/4\pi\}dV ,$$

where σ_n is the n-photon absorption cross section, $I(\mathbf{r})$ is the internal intensity of the incident wave, $\rho(\mathbf{r})$ is the density of molecules, and $F[\mathbf{r}, \theta_d, \mathbf{p}(\mathbf{E}^{\text{int}}(\mathbf{r}))]d\Omega/4\pi$ is the probability that a photon emitted from a molecule at $\mathbf{r}$ with its orientation along the $\mathbf{p}$ (dipole) axis reaches the detection aperture. Both $\mathbf{E}^{\text{int}}(\mathbf{r})$ and $F[\mathbf{r}, \theta_d, \mathbf{p}(\mathbf{E}^{\text{int}}(\mathbf{r}))]$ are dependent on the shape, size, and refractive index distribution of the microparticle and each must be integrated over the appropriate frequency bandwidth.

We calculate $U_n(\theta_d)$ for the specific case of a spherical liquid droplet containing uniformly dispersed dye molecules [$\rho(\mathbf{r}) = \rho_0$] which have a molecular rotation time much shorter than their fluorescence lifetime. Hence, $F[\mathbf{r}, \theta_d, \mathbf{p}(\mathbf{E}^{\text{int}}(\mathbf{r}))]$ is averaged over molecules having all orientations and can be written as $F(\mathbf{r}, \theta_d)$. To calculate $F(\mathbf{r}, \theta_d)$ for a sphere we expand the fields of the dipole in the vector spherical harmonics, match the boundary conditions at the surface [4,14], and normalize the frequency-integrated power collected from randomly oriented dipoles at $\mathbf{r}$ by the total frequency-integrated power emitted in all directions. This normalization differs from that used in [4] and means that smaller spheres can also be modeled. $E^{\text{int}}(\mathbf{r})$ is calculated by Fourier transforming the frequency-dependent fields (obtained at each frequency within the excitation spectrum using the Lorentz-Mie theory [3]). The excitation spectrum of the ultrashort incident pulse is assumed to be Fourier transform limited. In numerically integrating over frequency for both $F(\mathbf{r}, \theta_a)$ and $E^{\text{int}}(\mathbf{r})$ we use a finer integration step when near the morphology dependent resonances (MDRs, or whispering gallery modes). We define $I(\mathbf{r}) = \mathbf{E}^{\text{int}}(\mathbf{r})\,(\mathbf{E}^{\text{int}}(\mathbf{r}))^*$. The integration over the particle volume is performed using a Monte Carlo approach with more than 4×10^6 integration points for each angle θ_d.

Figure 1(a) shows the spatial distribution of $F(\mathbf{r}) = F(\mathbf{r}, \theta_d = 0°)$ in the equatorial plane, integrated over frequency and all dipole orientations. Figures 1(b) and 1(c) display $I(\mathbf{r})$, and $I^3(\mathbf{r})$, respectively. Because of reciprocity, $F(\mathbf{r})$ [rotated 180° from the orientation shown in Fig. 1(a)] and the $I^n(\mathbf{r})$ in 1(b) and 1(c) tend to be largest in the same regions, and so the largest $U_n(\theta_d)$ is found when $\theta_d = 180°$.

The experiments were performed on ethanol or methanol droplets containing Coumarin 510 dye. The droplets of 70 ± 10 μm diameter were produced with a piezodriven nozzle source, synchronized to the laser system so that each laser pulse excited one droplet. The droplet size

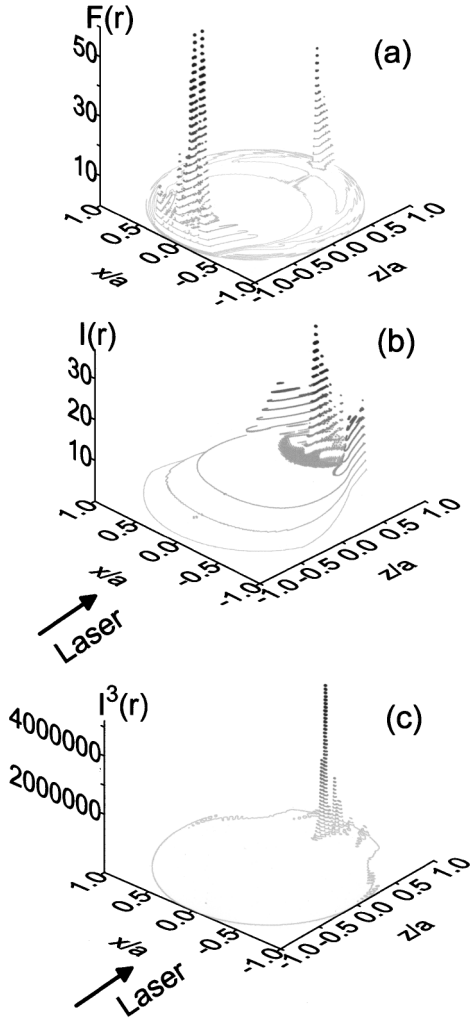

FIG. 1. Spatial distributions in the equatorial plane: (a) fraction of fluorescence collected at $\theta_d = 0°$, $F(\mathbf{r}) = F(\mathbf{r}, \theta_d = 0°)$, after integration over all dipole orientations. The molecular emission is centered at 510 nm (assumed Lorentzian with FWHM = 500 cm^{-1}); (b),(c) intensities $I(\mathbf{r})$ and $I^3(\mathbf{r})$, respectively. The center wavelengths and linewidths are 400 and 5 nm in (b), and 1200 and 15 nm in (c). The sphere diameter is $2a = 20$ μm, and its refractive index $m = 1.36 + i10^{-6}$.

and shape were monitored using a microscope and/or forward scattering of a He:Ne laser beam. The laser system consisted of a Kerr-lens mode-locked oscillator delivering 100 fs pulses, a 1 kHz Ti:sapphire regenerative amplifier, and an optical parametric amplifier. The use of ultrashort laser pulses has the advantage of depositing low energies in the particle and preventing competitive processes such as stimulated Brillouin scattering. The central wavelengths used for the one-, two-, and three-photon excitation of the microdroplets were 400, 850, and 1200 nm, respectively. Incident intensities were adjusted, depending on the order of the excitation process, to be 10 times below the measured saturation values (typically 6 kW/cm^2 at 400 nm, 2 GW/cm^2 at 850 nm, and 100 GW/cm^2 at 1200 nm). Emission spectra of both oscillator and amplifier outputs were monitored with a spectrometer and a

charge-coupled device camera, and the pulse duration of the amplified output was determined with an autocorrelator. The angular distribution of the far field fluorescence intensity, which peaks at 510 nm, was measured between $\theta_d = 0°$ (forward) and $\theta_d = 180°$ by using a photomultiplier tube (PMT) mounted onto a stepper-motor driven goniometer (with an angular resolution of 0.6°). A dichroic beam splitter was added for the near-backward direction measurements. The unwanted scattering of the pump radiation was reduced by using filters and by the very low quantum efficiency of the PMT at 850 and 1200 nm.

Figure 2 shows both experimental and theoretical results for the one-, two-, and three-photon excitation of the microdroplet fluorescence. These results constitute the first observation of a strongly asymmetric spontaneous emission from a multiphoton-excited spherical microcavity. Both results demonstrate the remarkable effect that the maximum of the incoherently emitted light is in the direction towards the exciting source, and that this enhancement strongly increases with the order of the multiphoton process. The backward enhancement of the emission was found in computations to increase as the refractive index of the microsphere increases, because the fields are more concentrated for larger m.

The experimental data were obtained on different days over several months, which demonstrates the good reproducibility of the experiment. The standard deviation, resulting from noise, laser power variations, and droplet stream stability is typically 0.2. We verified that the 2PEF and 3PEF processes were proportional to $I^2(\mathbf{r})$ and $I^3(\mathbf{r})$, respectively. The agreement between theory and experiment is remarkable even though the droplet diameter used in the experiments was 70 ± 10 μm and in the calculations was 20 μm, due to CPU-time limitations. Computationally, the dependence of the angular distribution on size was investigated (discussed below) and found to be nearly size independent for diameters >6 μm. Both theory and experiment yield similar fluorescence intensity ratios $I(180°)/(90°)$, which are 1.8, 5, and 9 for the one-, two-, and three-photon excitation, respectively. Similar angular patterns were obtained experimentally for multiphoton excitation when the dye concentration was varied from 0.02 to 2 g/l. For linear excitation, only a weak asymmetry is observed in the backward direction. The steep rise in narrow angular range (10°) around $\theta_d = 180°$ for the measured two- and three-photon excited fluorescence agrees both qualitatively and quantitatively with theory.

Besides the observed asymmetry, the angular distribution was found to be remarkably smooth. The angular distribution of on-resonance elastic scattering exhibits many lobes commensurate with the MDR mode number. However, for the one-photon and multiphoton-excited fluorescence case, the volume integral of the product of $F(\mathbf{r}, \theta_d)$ and $I^n(\mathbf{r})$ averages out the MDR structures in the calculated angular distribution even for single frequency excitation of an input and/or output resonance (results not shown).

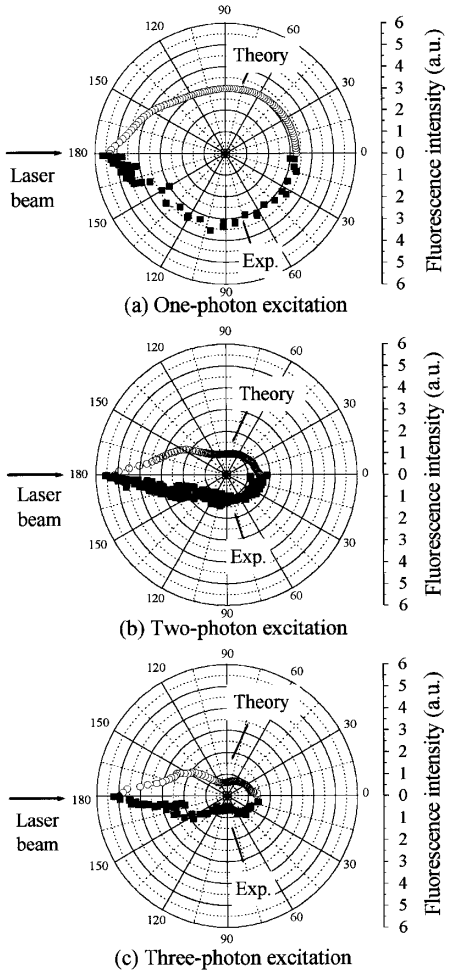

FIG. 2. Experimental and theoretical angular distributions of (a) one-, (b) two-, and (c) three-photon excited fluorescence from microdroplets made of ethanol ($m = 1.36 + i10^{-6}$) in (a) and (b), and methanol ($m = 1.325 + i10^{-6}$) in (c), and containing Coumarin 510. For the calculations the excitation center wavelength is 800 nm and the linewidth is 5 nm in (b), and the other wavelengths, linewidths, and diameter are as in Fig. 1. The calculated and experimental curves are normalized at $\theta_d = 90°$.

The effect of the size on the angular distribution was investigated computationally. Figure 3 shows the ratio $I(180°)/I(90°)$ for one-, two-, and three-photon excited fluorescence with increasing droplet diameter from 0.5 to 20 μm. This ratio approaches a constant for particles with diameters beyond 6 μm. Therefore, we can expect that using the calculated angular distribution results for 20-μm-diameter particles should be applicable for the experimental droplets of 70 μm in diameter. This is confirmed by the agreement between theory and experiment (see Fig. 2). Another observation of a convergence to specific values (the angles of peak emission of third harmonic generation) was reported for 16- to 64-μm-diameter droplets [15].

In summary, we propose that, because of reciprocity, MPEF from many shapes of dielectric microcavities or

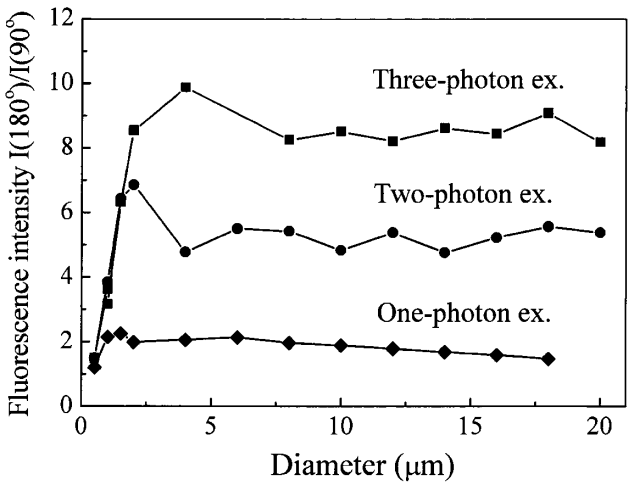

FIG. 3. Size dependence of the $I(180°)/I(90°)$ calculated for droplets with diameters from 0.5 to 20 μm. Other parameters are as in Fig. 2.

particles will be enhanced in the backward direction, and the backward enhancement will increase with the order n of multiphoton excitation. We verified this hypothesis both theoretically and experimentally for spherical dielectric microcavities. Measured and calculated angular distributions of emission have similar shapes and constitute the first observation of a strongly asymmetric angular distribution of the MPEF from a microcavity. The $I(180°)/I(90°)$ increases with the order of multiphoton process reaching a ratio of 9 for $n = 3$ excitation. The backward enhancement should be larger for particles having a larger refractive index.

J. P. W. acknowledges NATO's support. Y.-L. P. acknowledges financial support from the Army Research Laboratory (ARL, DAAL01-98-C0056). S. H. and R. K. C. acknowledge partial financial support from the U.S. Army Research Office (DAAG55-97-1-0349), the Air Force Research Laboratory, and ARL (DAAL01-97-2-0128).

[1] J. A. Lock and E. A. Hovenac, J. Opt. Soc. Am. A **8**, 1541 (1991).
[2] J. P. Barton, Appl. Opt. **34**, 5542 (1995).
[3] P. W. Barber and S. C. Hill, *Light Scattering by Particles: Computational Methods* (World Scientific, Singapore, 1990), pp. 140, 233.
[4] S. C. Hill, H. I. Saleheen, M. D. Barnes, W. B. Whitten, and J. M. Ramsey, Appl. Opt. **35**, 6278 (1996).
[5] R. F. Harrington, *Time-Harmonic Electromagnetic Fields* (McGraw-Hill, New York, 1961), pp. 116–125.
[6] S. C. Hill, G. Videen, and J. D. Pendleton, J. Opt. Soc. Am. B **14**, 2522 (1997).
[7] S. D. Druger and P. J. McNulty, Phys. Rev. A **29**, 1545 (1984).
[8] S. Maiti, J. B. Shear, R. M. Williams, W. R. Zipfel, and W. W. Webb, Science **275**, 530 (1997).
[9] X. D. Fan, S. Lacy, and H. L. Wang, Opt. Lett. **24**, 771 (1999).
[10] N. Lermer, M. D. Barnes, C. Y. Kung, W. B. Whitten, and J. M. Ramsey, Anal. Chem. **69**, 2115 (1997).
[11] V. Sandoghdar, F. Treussart, J. Hare, V. Lefevre-Seguin, J. M. Raimond, and S. Haroche, Phys. Rev. A **54**, 1777 (1996).
[12] H. Yukawa, S. Arnold, and K. Miyano, Phys. Rev. A **60**, 2491 (1999).
[13] D. S. Wiersma, M. P. van Albada, and A. Lagendijk, Phys. Rev. Lett. **75**, 1793 (1995).
[14] H. Chew, P. J. McNulty, and M. Kerker, Phys. Rev. A **13**, 396 (1976).
[15] J. Kasparian, B. Kramer, S. Vajda, P. Rairoux, B. Vezin, V. Boutou, T. Leisner, W. Hubner, J. P. Wolf, L. Woste, and K. H. Bennemann, Phys. Rev. Lett. **78**, 2952 (1997).